Antarctic Science 25(3), 397–408 (2013) © Antarctic Science Ltd 2012 doi:10.1017/S0954102012000909

The first record of fossil penguins from East Antarctica

PIOTR JADWISZCZAK[1], KRZYSZTOF P. KRAJEWSKI[2], ZINAIDA PUSHINA[3], ANDRZEJ TATUR[4] and GRZEGORZ ZIELIŃSKI[5]

[1]*Institute of Biology, University of Białystok, Świerkowa 20B, 15-950 Białystok, Poland*
[2]*Institute of Geological Sciences, Polish Academy of Sciences, Research Centre in Warszawa, Twarda 51/55, 00-818 Warszawa, Poland*
[3]*All-Russia Research Institute for Geology and Mineral Resources of the World Ocean (VNIIOkeangeologiya), Angliyskiy Prospekt 1, 190121 St Petersburg, Russia*
[4]*Faculty of Geology, Warsaw University, Żwirki i Wigury 93, 02-089 Warszawa, Poland*
[5]*Polish Geological Institute - National Research Institute, Rakowiecka 4, 00-975 Warszawa, Poland*
piotrj@uwb.edu.pl

Abstract: This paper presents the first fossil penguin from East Antarctica, and the only one known south of the Antarctic Circle. It is represented by two well-preserved elements of the wing skeleton, humerus and radius, obviously assignable to the extant genus *Spheniscus*. They were found in the glaciomarine succession of the Fisher Bench Formation (Fisher Massif, Prince Charles Mountains, Mac. Robertson Land), which was dated using Strontium Isotope Stratigraphy to be Late Miocene in age (10.2 Ma). They are only slightly younger than the oldest remains undoubtedly attributable to this taxon. The X-ray diffraction and Fourier Transform Infrared Spectroscopy indicate diagenetic alteration of the original bone bioapatite under dominantly marine conditions. The Late Miocene was a period of ice margin retreat and marine incursion into the Lambert embayment that followed Middle Miocene cooling of the Antarctic climate. The fossils strongly suggest that variable climatic and environmental conditions in East Antarctica may have been an important factor in the evolution of penguins there during the Neogene.

Received 20 April 2012, accepted 7 September 2012, first published online 15 November 2012

Key words: bioapatite diagenesis, Fisher Massif, Late Miocene, Prince Charles Mountains, *Spheniscus*, wing skeleton

Introduction

Penguins (Aves: Sphenisciformes) are a very distinct and relatively well-studied group of seabirds. Nevertheless, despite recent advances made in New Zealand (e.g. Slack *et al*. 2006), western South America (e.g. Clarke *et al*. 2010) and West Antarctica (e.g. Acosta Hospitaleche & Reguero 2010), their evolution is still poorly understood. The origin of this taxon is probably rooted in the Cretaceous (Slack *et al*. 2006), although the oldest fossils attributed to sphenisciforms come from the Early Paleocene of New Zealand, only 3–4 million years after the Cretaceous/Palaeogene transition (Slack *et al*. 2006). The most extensive fossil penguin collections ever, amounting to thousands of specimens, were acquired from the Eocene (56.0–33.9 Ma) sediments on Isla Marambio (Seymour Island), Antarctic Peninsula (Jadwiszczak 2006). Penguins of modern aspect appeared during the Miocene epoch (23.0–5.3 Ma), and some of them were attributed to extant genera (Göhlich 2007, Stucchi 2007, Jadwiszczak 2009, and references therein). The oldest named representative of this subgroup is *Spheniscus muizoni* Göhlich, 2007 from the Middle/Late Miocene (13.0–11.0 Ma) of Peru (Göhlich 2007).

Almost the whole evolutionary history of Sphenisciformes can be superimposed upon the global cooling trend through the Cenozoic, with episodes of more or less pronounced intermittent warming (Zachos *et al*. 2001). Interestingly, the only record of Antarctic fossil penguins discovered so far exists in the Late Paleocene–latest Eocene of Isla Marambio near the tip of the Antarctic Peninsula in West Antarctica. It is particularly abundant within the strata close to the Eocene/Oligocene transition, reflecting the onset of continental glaciation (Jadwiszczak 2006). This paper presents the Neogene (Late Miocene) sphenisciform remains revealed in the Prince Charles Mountains, Mac. Robertson Land in East Antarctica. Since they are post-Eocene in age and comprise the entire fossil record of Sphenisciformes known from both the eastern part of the continent and south of the Antarctic Circle, these bones are of real importance in improving our understanding of the evolution of penguins.

Geological setting

Antarctic glaciation has waxed and waned during the Cenozoic and distal correlations suggest that ice-volume changes have affected sea level (e.g. Frakes *et al*. 1992). Several marine incursions and glacier advances are recognized in the Cenozoic sediments exposed in the Prince Charles Mountains (Mac. Robertson Land, East Antarctica; Fig. 1), where they crop out over a series of nunataks and mountains along the west rift margin of the

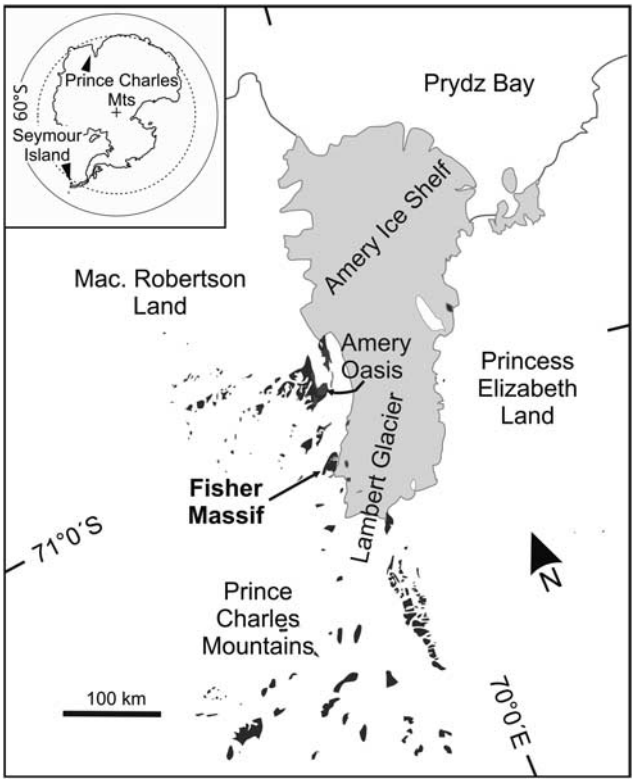

Fig. 1. Location map of the Fisher Massif in East Antarctica (based on a map from the Antarctic Digital Database, http://www.add.scar.org:8080/add, accessed November 2011).

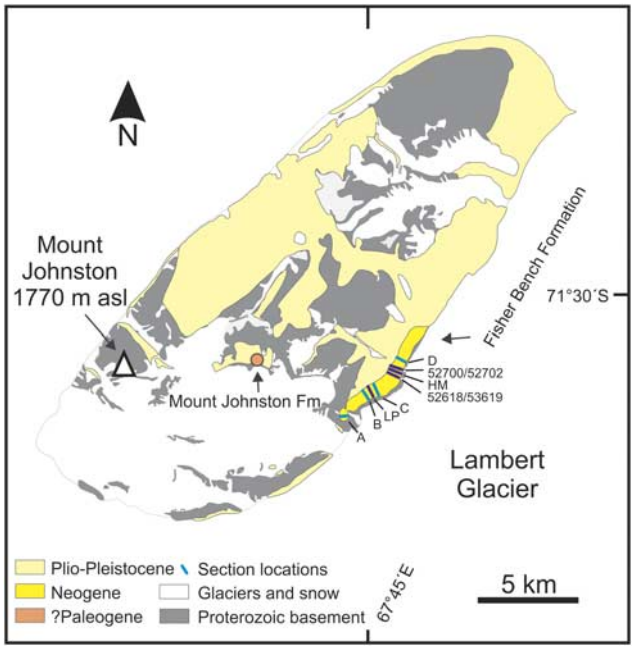

Fig. 2. Schematic map of the Fisher Massif in the Prince Charles Mountains (based on a map from the Antarctic Digital Database, http://www.add.scar.org:8080/add, accessed November 2011). Key to section abbreviations: A–D: this paper (after S. Ostrowski & M. Gola, unpublished data), LP: Layba & Pushina 1997, HM: Hambrey & McKelvey 1991, 52700/52702 and 52618/53619: Pushina *et al*. 2011.

Lambert Graben (Whitehead *et al*. 2006a). Cenozoic deposits of the Prince Charles Mountains are referred to as the Pagodroma Group (McKelvey *et al*. 2001). All published data from the Prince Charles Mountains refer only to two localities with Cenozoic glaciomarine diamict. The first is the Fisher Massif where the Mount Johnston and Fisher Bench formations occur. The second locality is in the Amery oasis (unofficial name) with the Battye Glacier and Bartin Bluff formations (Whitehead *et al*. 2004, Pushina *et al*. 2011).

The earliest (35–33 Ma) marine and glaciomarine deposits, containing *in situ* and/or glacially reworked diatoms, occur in the Mount Johnston Formation, Fisher Massif (Whitehead *et al*. 2004). They have been interpreted as representing reworked residues of the Late Eocene–Early Oligocene transgressive depositional system (O'Brien *et al*. 2001). However, unambiguously *in situ* diatom assemblages in glaciomarine sediments post-dated the Middle Miocene rapid cooling and massive build-up of ice cover in East Antarctica, the event often referred to as the Middle Miocene Climatic Transition (MMCT). During the MMCT, as demonstrated by Mg/Ca data from planktonic foraminifera, southern Pacific sea surface temperatures cooled 6–7°C (Shevenell *et al*. 2004) and tundra disappeared from terrestrial ecosystems in the McMurdo Dry Valleys due to rapid expansion of glaciers between 14.2 and 13.8 Ma (Lewis *et al*. 2008). A discontinuous record of sediments bearing *in situ* diatom assemblages (younger than that cooling event) was reported by many authors from the Pagodroma Group (for a critical review, see Whitehead *et al*. 2006b and Pushina *et al*. 2011).

The Proterozoic metamorphic and Permian–Triassic sediments form the basement to Neogene glacial and glaciomarine sediments of the Pagodroma Group (up to 370 m thick), interpreted to represent uplifted palaeofjord floor deposits. The sedimentary environment has been hypothesized to resemble those of the modern fjords of East Greenland (Whitehead *et al*. 2003). According to Whitehead *et al*. (2004), most of the Middle and Late Miocene Pagodroma Group consists of ice-proximal glaciomarine diamict with a subordinate admixture (< 2%) of ice-distal mudstone containing at places dispersed broken shells and diatom flora. The presence of marine diatoms enables biostratigraphic dating of the Late Miocene Pagodroma Group by comparing the diatom patterns elaborated from submarine coring in the Southern Ocean (mainly Kerguelen Plateau; see Whitehead *et al*. 2006b). Thin layers of fine-grained marine clastic sediment incorporated into the glacial diamictic succession of the Pagodroma Group mark the periods of ice margin retreat and marine incursion into the Lambert embayment.

https://doi.org/10.1017/S0954102012000909 Published online by Cambridge University Press

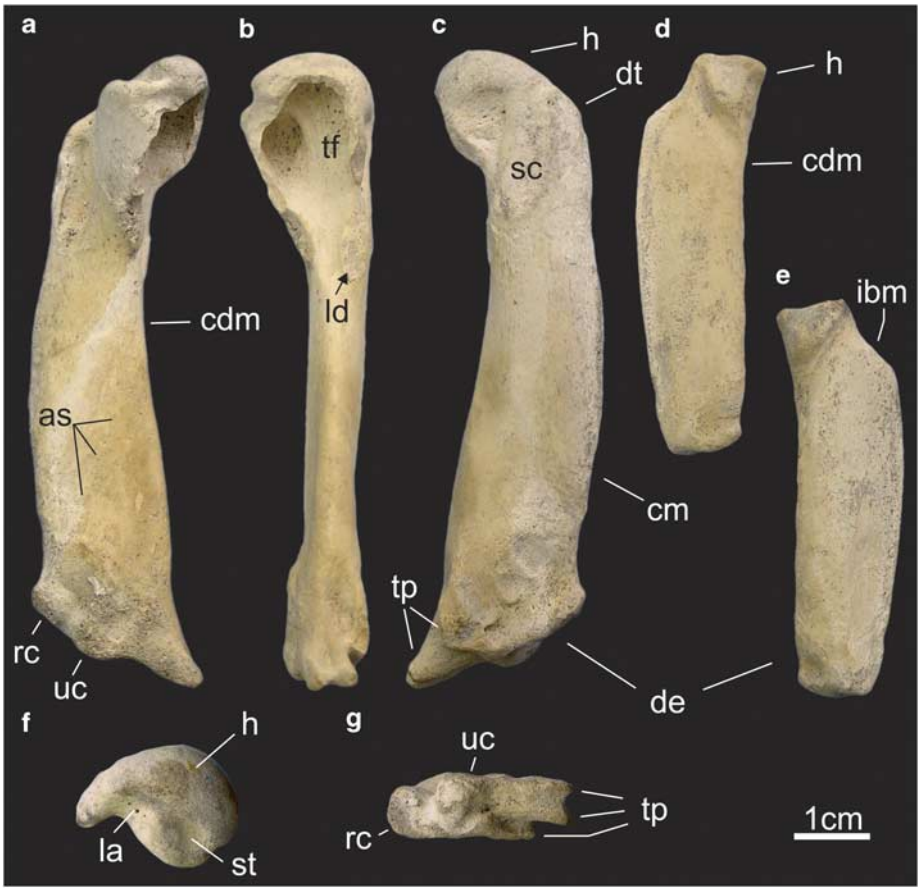

Fig. 3. Wing bones of the penguin from the Fisher Bench Formation in the Prince Charles Mountains: right humerus (**a.** ventral, **b.** caudal, **c.** dorsal, **f.** proximal, and **g.** distal view) and left radius (**d.** dorsal, and **e.** ventral view). Abbreviations: as = arterial sulcus, cdm = caudal margin, cm = cranial margin, de = distal end, dt = dorsal tubercle, h = head, ibm = insertion of brachial muscle, la = pit for ligament attachment (a crown-group feature), ld = attachment surface for latissimus dorsi muscle, rc = radial condyle, sc = attachment surface for supracoracoideus muscle, st = sulcus for transversal ligament, tf = tricipital fossa, tp = trochlear processes, uc = ulnar condyle.

Material and methods

Fieldwork

The Fisher Massif (Prince Charles Mountains; Figs 1 & 2) was the subject of regular geological investigations by the Russian-Polish team working during the 53rd Russian Antarctic Expedition in 2008. Several profiles of glacial and glaciomarine sediments in at least 350 m thick Miocene Fisher Bench Formation with many shell hash levels were logged and sampled in detail. The shell hash is here referred to as a mixture of sand or mud with gravel and unconsolidated broken shell material making horizons in the glaciomarine succession, which locally may be hardened due to increase of the shell number and the size of shell debris (shell banks).

Two well-preserved fossil penguin bones (Fig. 3) and a single shell of a pectenoid resembling the Recent Antarctic scallop, *Adamussium colbecki* (Smith, 1902) (Fig. 4), were found in the shell bank horizon cropping out at the lowest part of the Fisher Bench Formation, along the south-eastern edge of the Fisher Massif, at 330 m above sea level (a.s.l.) (Fig. 2). The bones were collected in close proximity to each other (1–2 cm) by the field team led by Dmitry Bolshiyanov. The hosting sediments were deposited in a marine environment without influence of ice shelf or outlet glaciers. They form a four-metre-thick sandy layer with abundant broken shells of *Hiatella* sp. and pectenoids (only a single shell was perfectly preserved, see Fig. 4). This agglomeration was formed during an open-sea incursion in the area of the Prince Charles Mountains and currently is located nearly 300 km landward from the permanent ice-edge (Bolshiyanov, unpublished data).

Several thin glaciomarine sediment horizons were recognized in sections (A, B, C, D) of glacial diamict of the Fisher Bench Formation (Fig. 2). A few of these horizons contain dispersed shell hash. Specimens collected from them were analysed by Strontium Isotope Stratigraphy method.

Palaeontological material

Fossil penguin bones recovered from the shell bank preserved morphological details that allow comparison with other fossil and Recent specimens. All skeletal elements, which include a complete left radius and an almost complete right humerus (Fig. 3), are permanently deposited at the Institute of Biology, University of Białystok (Poland), in the collection of the Andrzej Myrcha University Museum of Nature; abbreviated IB/P/B (IB/P/B-0965 for humerus and IB/P/B-0966 for radius). The pectenoid shell (Fig. 4) is housed at the Institute of Palaeobiology of the Polish Academy of

https://doi.org/10.1017/S0954102012000909 Published online by Cambridge University Press

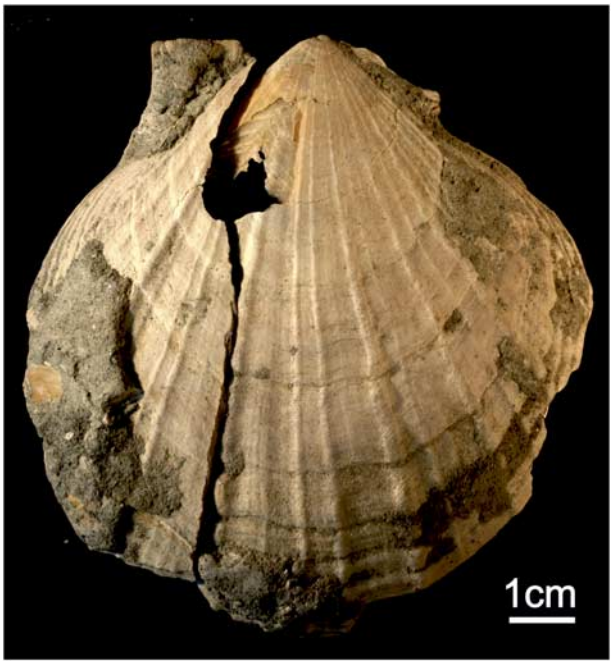

Fig. 4. Pectenoid shell (cf. *Adamussium colbecki* (Smith, 1902)) from the Fisher Bench Formation in the Prince Charles Mountains - a source of samples for the Strontium Isotope Stratigraphy method (picture courtesy of Andrzej Gaździcki).

Sciences in Warsaw. Measurements (for definitions, see Table I) were taken using digital callipers and rounded to the nearest 0.1 mm.

Mineralogical analysis of the penguin bone apatite

The X-ray diffraction (XRD) and Fourier Transform Infrared Spectroscopy (FTIR) are commonly used to assess diagenetic alteration of the original bone material (e.g. Person *et al*. 1995, 1996). In both methods, the Crystallinity Index (CI) is a measure of the degree of order within the bioapatite structure, which is a function of crystal size, its composition, and structural defects (Surovell & Stiner 2001, Munro *et al*. 2007).

The mineralogy of bioapatite in the radius of a fossil penguin (Fig. 3) from the Fisher Bench Formation (Prince Charles Mountains) was analysed by means of XRD and FTIR. The sample was drilled from the central part of the bone using a standard dental drill. This sample is referred to as 'Penguin bone PChMts' in the present paper. For comparative purposes two other samples of bio- and hydroxyapatite were analysed using the same methods and instrumental parameters. These were a synthetic hydroxyapatite from chemical industry and a bioapatite in the subfossil wing bone of *Pygoscelis adeliae* (Hombron et Jacquinot, 1841) collected at penguin rookery in Admiralty Bay, King George Island, West Antarctica. These samples are referred to as 'Hydroxyapatite' and 'Subfossil penguin bone KGI', respectively.

For XRD analysis the samples were ground to $< 63\,\mu m$ fraction. Diffraction patterns were recorded on a Sigma 2070 diffractometer (CGR, France) using a curved position sensitive detector in the range 2–120° 2Θ with CoKα radiation. The detector channels were calibrated with an external standard composed of a mixture of tetradecanol, böhmite, and silicon. The calibration was verified using quartz lines at 3.345, 1.817, and 1.541 Å. Diffractionel software v. 03/93 (Inel Instrumentation Electronique, France; http://www.inel.fr) was used to process the obtained data. The analysis was done at the Institute of Geological Sciences, Polish Academy of Sciences in Warsaw. The Crystallinity Index of bio-/hydroxyapatite in the XRD patterns (XRD CI) was calculated using the equation of Person *et al*. (1995): XRD CI = Σ{H[202], H[300], H[112]}/H[211], where H is the height of peaks corresponding to reflections [211], [112], [300], and [202]. The height was measured between the average value at the top of a peak and a local baseline drawn between 28° and 44° 2Θ.

The FTIR spectra were obtained using KBr pellets pressed under vacuum (1:60 mixture of ground sample and KBr). The spectra were recorded with a Perkin Elmer System 2000 spectrometer in terms of absorbance versus wave number ν in the range 400–4000 cm^{-1}. The analysis was done at the Industrial Chemistry Research Institute in Warsaw. The Crystallinity Index of bio-/hydroxyapatite in FTIR spectra (FTIR CI) were calculated according to the method presented by Munro *et al*. (2007): FTIR CI = $(h\,A_{565cm\text{-}1} + h\,A_{602cm\text{-}1})/h_{588cm\text{-}1}$, where $h\,A_{565cm\text{-}1}$ and $h\,A_{602cm\text{-}1}$ are the heights of the ν_4 PO_4^{3-} antisymmetric bending frequencies at approximately 565 cm^{-1} and 602 cm^{-1}, and $h_{588cm\text{-}1}$ is the height of the enclosed valley at 588 cm^{-1}, related to a local baseline drawn between 750 cm^{-1} and 450 cm^{-1}.

Strontium Isotope Stratigraphy

The age of penguin bones was indirectly (see below) estimated using Strontium Isotope Stratigraphy (SIS) (e.g. Howarth & McArthur 1997). The SIS analysis was performed after geochemical testing of shells (C and O isotopic analysis, XRD, Atomic Emission Spectrometry with Inductively Coupled Plasma [AES-ICP], and Scanning Electron Microscopy (SEM)) proving that they are suitable for isotopic analysis. Determinations of $^{87}Sr/^{86}Sr$ isotopic ratios in low-Mg biogenic calcite were performed on the perfectly preserved shell of a pectenoid bivalve (Fig. 4) that was found in close proximity to the penguin bones, within the shell bank near the base of the Fisher Massif Formation. Strontium Isotope Stratigraphy analyses were also performed on shell fragments collected from every shell bearing horizon recognized in sections A, B and C of the Fisher Bench Formation. Geochemical tests preceding these analyses were restricted to XRD and SEM.

Shell fragments for the SIS analysis were separated under an optical microscope (binocular), rinsed with the

https://doi.org/10.1017/S0954102012000909 Published online by Cambridge University Press

Table I. Measurements (in mm) of humeri and radii of fossil and extant penguins. Compiled from Stephan 1979, Emslie & Correa 2003, and Göhlich 2007. Abbreviations: L = length between humeral head and ulnar condyle, PW = proximal width, LW = least width, GDW = greatest distal width, GL = greatest length, DW = distal width. Number of specimens in parentheses (preceded by mean and range).

Species	Humerus					Radius	
	L	PW	LW	GDW	GL	PW	DW
Fossil penguins							
PChMts penguin (this study)	81.4	21.7	14.0[1]	25.8	53.4	9.9[2]	10.0
Spheniscus muizoni	70.2 69.6–70.9 (2)	22.8 22.6–22.9 (2)	13.2 13.1–13.4 (2)	24.0	47.7	8.1	6.6
Spheniscus urbinai	99.2 85.9–108.0 (42)						
Spheniscus chilensis	70.2 68.2–72.2 (5)	20.3 18.1–22.3 (5)	11.9 10.1–12.5 (7)				
Extant penguins							
Spheniscus mendiculus	57.0 56.0–58.8 (3)	16.7 16.6–16.8 (3)					
Spheniscus magellanicus	69.3 65.3–73.2 (6)	20.0 19.2–20.8 (4)	11.5 11.0–11.8 (4)	23.2 22.1–24.3 (4)	48.2 46.8–50.1 (4)	8.2 8.0–8.4 (4)	7.9 7.8–8.2 (3)
Spheniscus humboldti	71.5 68.6–74.3 (13)	21.3 20.0–22.0 (3)	12.7 12.2–13.6 (3)	24.3 23.0–25.0 (3)	48.9 48.6–49.2 (3)	8.8 8.5–9.0 (3)	8.9 8.8–9.0 (3)
Spheniscus demersus	66.9 62.0–73.6 (16)	19.2 18.0–20.2 (8)	11.1 10.2–11.6 (8)	23.0 22.1–23.5 (8)	47.1 44.4–51.2 (8)	8.3 7.8–9.0 (7)	7.6 6.0–8.2 (6)
Pygoscelis papua	81.1 75.0–88.2 (8)	21.2 19.4–23.0 (8)	15.1 14.0–16.6 (8)	26.2 24.2–28.2 (8)	56.8 51.8–62.5 (8)	10.0 9.0–10.5 (8)	10.0 9.0–10.6 (8)

[1] Midshaft width: 15.7.
[2] Midshaft width: 14.2.

UHQ-class water in a ultrasonic bath, dried and powdered in an agate mortar. The Suprapur-class acetic acid and UHQ-class deionized water was used for the chemical separation. Weighed subsamples of *c.* 50 mg of a powdered sample were dissolved in 1 ml 2 M Suprapur-class acetic acid. After 24 hours, they were centrifuged, and the residue (if detected) was removed. The solutions were evaporated (twice, to dryness) from the Suprapur-class hydrochloric acid, and dissolved in 2.5 M hydrochloric acid. The column chromatography was a two-step procedure, using both ion-exchange (Bio-Rad X82) and Sr-selective (Sr spec.) resin. Sr fractions were evaporated to dryness from the Supra-class nitric acid (with a drop of phosphoric acid), and in this form placed on the tantalum filament. The measurement of the isotopic composition was carried out using a mass spectrometer VG Sector 54 at the Isotope Geochemistry Laboratory of the Institute of Geological Sciences (Polish Academy of Sciences) in Krakow. The following settings were used: mode - multicollector dynamic, ion beam current - 3 V, number of replications for a single sample - 100. The results were normalized relative to the istopic standard NIST SRM 987 for the isotopic ratio reference value $^{87}Sr/^{86}Sr = 0.710250$.

Systematic palaeontology

Aves L., 1758
Sphenisciformes Sharpe, 1891 (also *sensu* Clarke *et al*. 2003)
Spheniscidae *sensu* Clarke *et al*. 2003

Remarks. The Linnean family name Spheniscidae Bonaparte, 1831 was applied by Clarke *et al*. (2003) to the clade comprising the most recent common ancestor of all extant penguins and all of its descendants. According to the above-mentioned approach, this group includes not only

https://doi.org/10.1017/S0954102012000909 Published online by Cambridge University Press

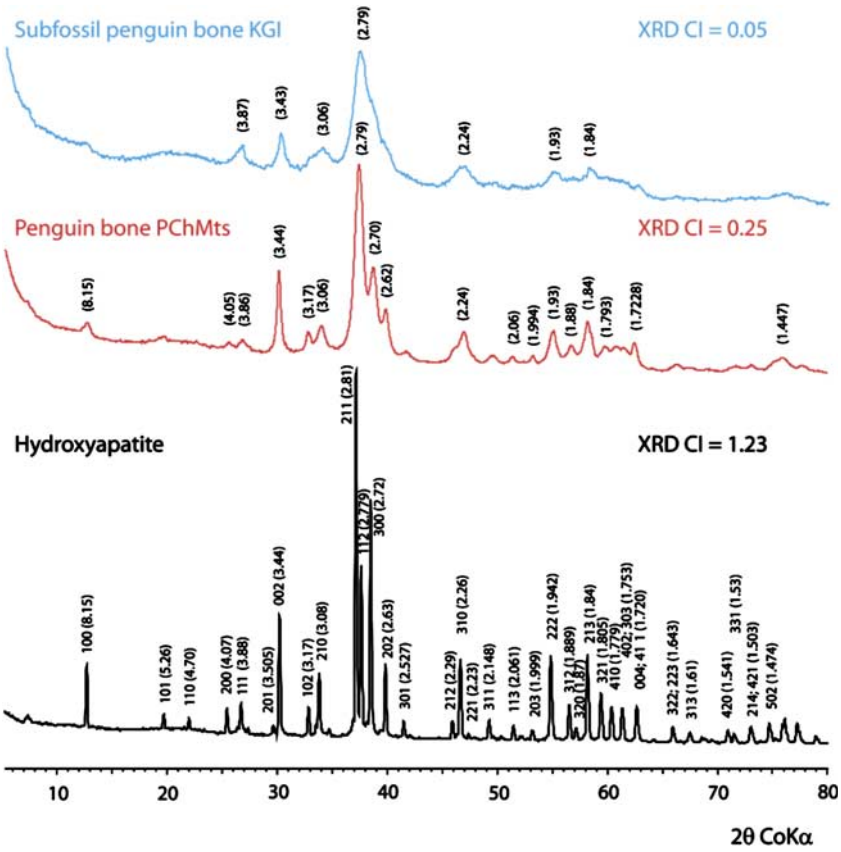

Fig. 5. X-ray diffractograms (XRD) of a penguin radius from the Fisher Bench Formation in the Prince Charles Mountains (penguin bone PChMts) and two reference samples (hydroxyapatite and subfossil penguin bone KGI). Numbers indicate *hkl* reflections of hydroxyapatite. In brackets there are indicated the values of spacing (*d*) of lattice planes of bio-/hydroxyapatite (in angstroms, Å). XRD CI is the crystallinity index. For other explanations, see text.

17 modern-day sphenisciform species grouped into six genera (Jadwiszczak 2009), but also at least seven Miocene and Pliocene species from both extant (*Pygoscelis grandis* Walsh et Suarez, 2006, *Spheniscus muizoni*, *Spheniscus megaramphus* Stucchi *et al.*, 2003, *Spheniscus urbinai* Stucchi, 2002) and extinct (*Nucleornis insolitus* (Simpson, 1979), *Madrynornis mirandus* Acosta Hospitaleche *et al.*, 2007, *Inguza predemersus* (Simpson, 1971)) genera (Ksepka & Thomas 2012, fig. 2). The only humeral feature that characterizes these penguins (crown group penguins) reported by Ksepka & Thomas (2012) is the presence of a pit for ligament insertion on a proximal surface adjacent to the head. In specimen IB/P/B-0965 such a pit is noticeable though shallow, comparable to that in *Spheniscus magellanicus* (Forster, 1781) (PJ, personal observation and Fig. 3).

Genus *Spheniscus* Moehring, 1758

Remarks. The following set of humeral characters was reported by Göhlich (2007) as diagnostic for *Spheniscus* penguins: i) head barely swollen proximally, ii) proximal outline of bone without notch between dorsal tubercle and the head, iii) proximal-most trochlear process ("caudal-most process of the ventral epicondyle" in Göhlich 2007) hardly surpassing caudal ("ventral" in Göhlich 2007) margin of distal shaft, iv) bipartite tricipital fossa with a deep ventral ("cranial" in Göhlich 2007) fossa, and v) proximal border of tricipital fossa straight and almost horizontal in caudal view ("ventral view" in Göhlich 2007). Of these, three features (i, ii and iv) are conspicuous in specimen IB/P/B-0965 (Fig. 3). The degree of confidence is lower in the case of the trochlear process (iii) - since its tip is broken, the actual shape must have been estimated. In our opinion, however, it had not protruded far beyond the shaft margin (as is typical of *Spheniscus*). Additionally, tips of two distal-most trochlear processes are subequal in their lengths (in distal view; Fig. 3g), which in our estimation may be an apomorphy of the *Spheniscus* (PJ, personal observation; Stephan 1979, fig. 36; Göhlich 2007, fig. 4). The fifth feature cannot be analysed because the bone discussed here is missing too much of the relevant part (Fig. 3b). In fact, it does not appear to be of diagnostic value at generic level - even Göhlich (2007, p. 287) acknowledged a difference between a set comprising all extant *Spheniscus* species+*S. muizoni*, and *Spheniscus chilensis* Emslie et Guerra Correa, 2003 and *S. urbinai* in this respect.

Spheniscus sp.

Material. IB/P/B-0965 (almost complete right humerus) and IB/P/B-0966 (complete left radius) (Fig. 3).
Locality. Fisher Massif, Prince Charles Mountains, Mac. Robertson Land, East Antarctica (Figs 1 & 2).
Formation and age. Fisher Bench Formation (Fig. 2); 10.2 Ma, Late Miocene (for details, see SIS age estimation below).

https://doi.org/10.1017/S0954102012000909 Published online by Cambridge University Press

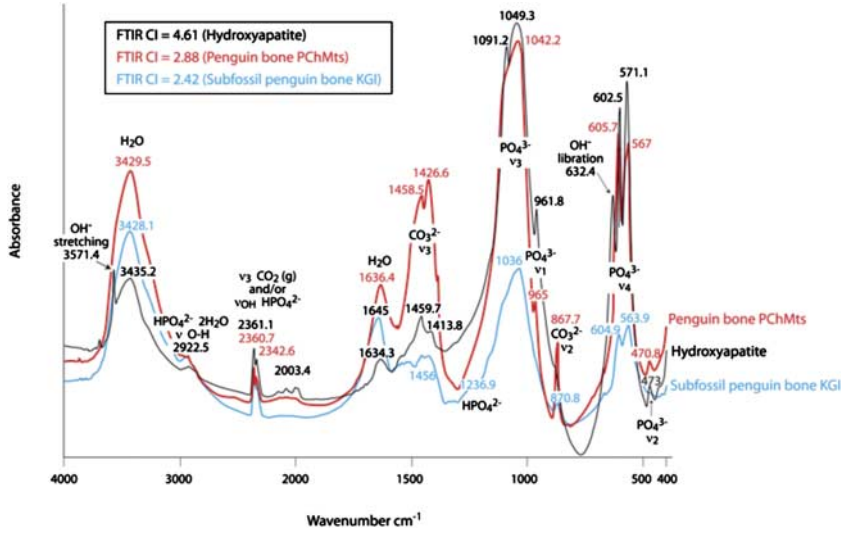

Fig. 6. Fourier Transform Infrared (FTIR) spectra of penguin radius from the Fisher Bench Formation in the Prince Charles Mountains (penguin bone PChMts) and two reference samples (hydroxyapatite and subfossil penguin bone KGI). FTIR CI is the crystallinity index. For other explanations, see text.

Description and comparisons. Both elements of the wing skeleton belonged to a medium-sized (relative to Recent sphenisciforms), most probably adult penguin. It was smaller than Miocene–Pliocene *S. urbinai* but larger than Miocene *S. muizoni*, Pliocene *S. chilensis* and representatives of its four extant congenerics; within the size range of Recent *Pygoscelis papua* (Forster, 1781) (Table I). In addition to the features mentioned above, the humeral shaft widens distally, the proximal outline from the humeral head to the cranial ("dorsal" in Göhlich 2007) margin is very steep (steeper than in other species). The transversal ligamental furrow (located just distal to the humeral head, close to the proximal margin of the tricipital fossa) forms a deep pit. Attachment surfaces for the supracoracoideus and latissimus dorsi muscles are well developed, the former is oblique, the latter ovoid. The bicipital crest is concave, but its indentation is probably not as distinct as in *S. muizoni* (Göhlich 2007, figs 2 & 4). The so-called preaxial angle of the shaft (i.e. an angular prominence of the preaxial border) is absent, although actually, since some degree of abrasion cannot be excluded, it could have been as weak as (or slightly weaker than) that in *S. muizoni* (Göhlich 2007, fig. 2). The humeral arterial sulcus (Thomas *et al*. 2010) is well developed. Above this structure, there is yet another conspicuous (although very narrow) sulcus incised obliquely into the ventral surface of the bone, such a structure is present (although barely detectable) in some present-day (e.g. *P. papua*) and fossil (e.g. *Palaeospheniscus bergi* Moreno et Mercerat, 1891) penguin humeri (PJ personal observation). The angle between the main axis of the shaft and the tangent or radial and ulnar condyles is 47° (according to Ksepka *et al*. 2006, values above 45° suit the general condition in penguins). The ulnar condyle is slightly rounded and the shelf adjacent to it is quite narrow. The radial condyle appears to be flattened.

The radius was found close to the humerus and is believed to represent the same individual. Its length constitutes 0.7 of humeral length (Table I), which is typical of both extinct and extant *Spheniscus* penguins. However, unlike the humerus it is practically of no diagnostic value. This is because the fossil radii are very similar to those belonging to extant species, the only point of interest being the insertion of the brachial muscle (between the radial head and cranial margin). The modern-type radii, also present in some extinct species, possess this attachment in a form of a more or less developed notch (PJ personal observation). This feature is not observed in the penguin from the Fisher Bench Formation, whereas *S. chilensis* and *S. muizoni* seem to represent the intermediate condition (Emslie & Correa 2003, fig. 2; Göhlich 2007, fig. 2). *Measurements*. See Table I.

Mineralogy and diagenesis of the PChMts penguin bone

The XRD pattern of the reference synthetic hydroxyapatite shows reflexes of all major lattice planes sharp and clearly separated, indicating a well-ordered crystal structure with XRD CI as high as 1.23 (Fig. 5). In contrast, the patterns of the analysed penguin bones show broad reflections associated with their partial overlap. The two main reflections of hydroxyapatite corresponding to lattice planes [211] and [112] (spacing 2.81 Å and 2.78 Å, respectively) overlap in the bioapatites to form one broad reflection with spacing $d = 2.79$ Å. However, bioapatite of the bone from Prince Charles Mountains shows partially separated reflections of lattice planes [300] and [202] (spacing 2.70 Å and 2.62 Å, respectively), which are hidden in the pattern of the subfossil bone from King George Island. Other major reflections, including lattice planes [002], [310], [222] and [213], are also far better pronounced in the Prince Charles Mountains sample. This is confirmed by a fivefold difference in the XRD CI between PChMts (0.25) and KGI (0.05) samples (Fig. 5).

The FTIR spectrum of the reference synthetic hydroxyapatite shows well-defined absorption bands

https://doi.org/10.1017/S0954102012000909 Published online by Cambridge University Press

Table II. Location of analysed samples and results of Strontium Isotope Stratigraphy analyses.

Sample ID	Base of profile altitude m a.s.l.	Basement at the base of profile yes/no	Profile thickness m	Sample position m above the base	$^{87}Sr/^{86}Sr$ ratio	Age Ma	± Ma	Average age Ma for horizon	Mineral composition
pectenoid					0.708846	11.45	0.4		calcite low-Mg
pectenoid	330 sampling site			few m above basement	0.708903	9.50	0.4	10.2	calcite low-Mg
pectenoid					0.708898	9.70	0.4		calcite low-Mg
A 1				74	0.708890	9.90	0.4		aragonite
	376	no	100					9.9	
A 1				74	0.708889	9.90	0.4		aragonite
B 15				0	0.708922	8.75	0.4	8.8	aragonite
B 19				77	0.708855	11.00	0.5	11.0	calcite low-Mg
B 20	373	yes	295	127	0.708932	8.15	0.4		aragonite
								8.3	
B 20				127	0.708927	8.50	0.4		aragonite
B 21				152	0.709124	1.20	0.5	1.2	aragonite
C 30				0	0.709270	< 0		< 1	aragonite
	328	yes	200						
C 33				48	0.709306	< 0		< 1	aragonite

corresponding to bending frequencies of PO_4^{3-} (ν_2 473 cm^{-1}, ν_3 1091 cm^{-1} and 1049 cm^{-1}, ν_4 603 cm^{-1} and 571 cm^{-1}), stretching band at ν_1 962 cm^{-1}, and structural OH^- libration band at 632 cm^{-1} and stretching band at 3571 cm^{-1} (Fig. 6). Absorption bands at 1634 cm^{-1} and 3435 cm^{-1} suggest the presence of adsorbed H_2O. The broad and indistinct bands at 1414 cm^{-1} and 1460 cm^{-1}, which reflect ν_3 CO_3^{2-} bending frequencies, indicate subordinate lattice substitution of PO_4^{3-} by CO_3^{2-}. The two bands at approximately 2361 cm^{-1} may be related to the adsorbed CO_2 and/or to ν_{OH} HPO_4^{2-} stretching frequencies (Panda *et al*. 2003). The FTIR spectra of bioapatite of the analysed penguin bones show very indistinct bands related to bending frequencies of structural OH^-. The FTIR spectrum of PChMts sample shows sharp bands of ν_1 (965 cm^{-1}) stretching, and ν_2 (471 cm^{-1}), ν_3 (1042 cm^{-1}) and ν_4 (606 cm^{-1} and 567 cm^{-1}) bending frequencies of PO_4^{3-}. Well-defined are bands of ν_2 (871 cm^{-1}) and ν_3 (1456 cm^{-1}) bending frequencies of CO_3^{2-} replacing PO_4^{3-} in the crystal lattice of bioapatite. The FTIR spectrum of KGI sample shows only two bands of bending frequency of PO_4^{3-}: ν_3 ($\sim$1036 cm^{-1}) and ν_4 (605 cm^{-1} and 564 cm^{-1}). The most prominent in this sample are two bands related to adsorbed H_2O and one related to absorbed CO_2 (1645 cm^{-1} and 3428 cm^{-1}, and $\sim$2361 cm^{-1}, respectively). The broad and complex band at $\sim$1520 cm^{-1} reflects the presence of organic matter. The FTIR CI values calculated for hydroxyapatite, and PChMts and KGI bioapatite samples are 4.61, 2.88 and 2.42, respectively (Fig. 6). The CI value for synthetic hydroxyapatite is greater than the range typical for recrystallized bone material. The values of penguin bones are within the range of modern bones, although the degree of crystallinity of PChMts sample is far better pronounced.

Strontium Isotope Stratigraphy age estimation

Strontium stable isotopes, determined in three independent samples from a single pectenoid (the low-Mg calcite shell), yielded the following $^{87}Sr/^{86}Sr$ ratios: 0.708898, 0.708903 and 0.708846. The mean isotopic age, inferred from these values according to the standard SIS curve (Howarth & McArthur 1997, McArthur *et al*. 2001), is 10.2 Ma, which corresponds to the Late Miocene (Table II).

Supplementary SIS analyses were performed on damaged shell fragments collected from seven shell bearing horizons recognized in the lower and middle part of the Fisher Bench Formation along sections A, B and C (Table II). Six samples (A 1, A 1a, B 15, B 19, B 20, B 20a) collected from four horizons, yielded $^{87}Sr/^{86}Sr$ ratios between 0.708855 and 0.708932 that suggest the Late Miocene age ranging from 8.3–11.0 Ma. Three samples (C 30, C 33, B 21) gave evidently false results that will be discussed in a paper under preparation. Most probably, the aragonitic debris analysed can be attributed to the marine bivalve genus *Hiatella*, whereas a single calcite shell (sample B 19) can be assigned to a pectenoid. These two bivalves, differing in mineral composition of their shells, occur in Miocene sediments from that region. All low-Mg calcite shells, probably belonging to pectenoids, gave ages ranging from 11.45–9.50 Ma, i.e. older than the ones obtained from aragonite shells of ?*Hiatella* sp. (9.90–8.15 Ma); unreliable values were rejected (see Table II).

Discussion

Geology and stratigraphy

The shell bank with fossil penguin bones and a well-preserved pectenoid was found within the lower part of Neogene

https://doi.org/10.1017/S0954102012000909 Published online by Cambridge University Press

glaciomarine sediments of the Fisher Bench Formation, at the altitude of 330 m a.s.l., a few metres above the crystalline basement (Bolshiyanov, personal communication 2008). Sandy matrix of this deposit was micropalaeontologically barren, and it was hardly possible to provide detailed description of the lithological profile at this place because of the slope steepness. Therefore, the stratigraphic position of the shell bank has been documented on the basis of diatoms obtained from geological sections located in the close vicinity (Fig. 2) and from the available SIS data (Table II). Several thin marine mudstone horizons were recognized in glaciomarine diamict of the Fisher Bench Formation, some of them contain diatom flora, but only few yielded diatoms that can be considered as *in situ* assemblages and only few contain shell hash (Table II).

During recent years, extensive geological studies were performed in the Prince Charles Mountains by the Russian Antarctic Expedition, providing new data on palaeoecology and chronology of the Neogene deposits that substantially extended the existing knowledge (Hambrey & McKelvey 1991, Layba & Pushina 1997, McKelvey *et al*. 2001, Whitehead *et al*. 2003, 2004, 2006a). Particular attention was paid to the Fisher Bench Formation, where important lithostratigraphic questions were not sufficiently explained. Among a large number of samples containing poorly preserved and reworked diatoms of mixed composition, Pushina *et al*. (2011) recognized the following sequence of horizons with *in situ* diatom assemblages:

i) Middle Miocene planktonic assemblage, recognized only in some sections at the base of the Fisher Bench Formation. It represents open marine conditions. The planktonic taxa (up to 95%) are represented by *Denticulopsis simonsenii* Yanagisawa and Akiba, 1990, *Actinocyclus ingens* Rattray, 1890, *Eucampia antarctica* (Castracane) Mangin, 1914, and *Melosira* sp. The first two species are stratigraphic markers in diatom zonation pointing to an age range between 12.1 and 11.5 Ma, that corresponds to the marine event M5 of Whitehead *et al*. (2006b).

ii) A Late Miocene benthic sublittoral assemblage, widespread in the lower and middle parts of the Fisher Bench Formation, that represents sublittoral environment dominated by benthic species (up to 78%): *Synedra* spp., *Navicula* sp., *Rhabdonema* spp. (planktonic species are also present). Some representatives of *Rhabdonema* and *Synedra* belong to new species, and probably represent the best *in situ* marker for the marine event M6 (10.7–8.5 Ma) of Whitehead *et al*. (2006b; presumably associated with warm climatic conditions).

iii) A freshwater assemblage widely dispersed throughout the upper part of the formation. It is characterized by high contribution of freshwater benthic diatoms (representing lacustrine environment) with many new endemic species (they are currently under elaboration; Pushina unpublished data). Unfortunately, it is not possible to determine the age of this unit on the basis of diatoms and seashells are absent in this part of the formation.

The shell bank bearing penguin bones is located at the base of a unit containing sublittoral diatoms, that followed an erosional episode (E3+ of Whitehead *et al*. 2006b) between 10.7 and 9.0 Ma (Whitehead *et al*. 2006b). This bank was probably formed due to wave action during storms, similarly to penguin bone bearing para-autochthonous shell accumulations in the Eocene La Meseta Formation on Isla Marambio (Myrcha *et al*. 2002). The SIS dating of the pectenoid shell (10.2 Ma) is consistent with the age suggested on the basis of diatom analysis (Table II). The ages estimated from aragonite shells (probably *Hiatella* sp.) from stratigraphically younger parts of the section are between 9.9 and 8.3 Ma, and they are consistent with the age range for the benthic diatom unit (10.7–8.5 Ma) estimated using diatom biostratigraphy. A slightly older age obtained for a single pectenoid shell from the middle part of the section (specimen B 19; see Table II) may suggest that it was reworked from the bottom part of the unit with benthic diatoms. Some results from aragonite shells (section C and the sample from the upper level) are evidently unreliable (Table II). It is plausible that input of freshwater to glaciated fjord and/or the affinity of some *Hiatella* populations to brackish water affected the isotopic composition of the shell strontium, thus giving false SIS dates. Moreover, aragonitic shells are considered as less valuable material for SIS dating than low-Mg calcite. Unreliable data with similar strontium isotope ratios were published from the Miocene deposits of the Prince Charles Mountains by Whitehead *et al*. (2004).

The penguin bones described here were found in sediments deposited during a period of warmer climate between 10.0 and 8.5 Ma (Billups & Schrag 2002), following the most important climate cooling in Antarctica coeval with the final opening of Drake Passage and the development of modern water circulation pattern in the Southern Ocean. The oceanic incursion event into the Lambert Graben recorded in the Fisher Bench Formation can be correlated with the marine onlap sequence Tor-1 in Tortonian, Late Miocene (11.70–9.32 Ma), which occurred during the highest global sea level reported for the Neogene (Snedden & Liu 2010).

Diagenetic modification

The XRD and FTIR analyses indicate that the penguin bone from the Fisher Bench Formation in the Prince Charles Mountains shows diagenetic recrystallization and neoformation compared to a subfossil bone. The XRD and FTIR CI values fall in the ranges typical for recrystallized and unaltered (modern) bones, respectively (Person *et al*. 1996, Huertas *et al*. 1997). The most pronounced diagenetic changes of the PChMts bone embrace an increase of crystal size, a loss

https://doi.org/10.1017/S0954102012000909 Published online by Cambridge University Press

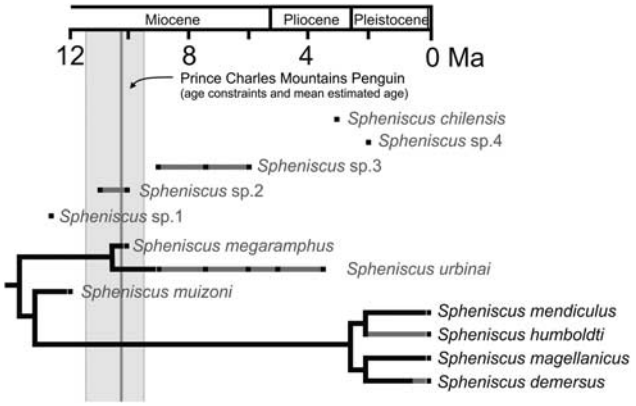

Fig. 7. Phylogeny of the genus *Spheniscus* (a compilation based on Emslie & Correa 2003, Göhlich 2007, Stucchi 2007, Jadwiszczak 2009, Ksepka & Thomas 2012, and data from this study). Fossil ranges are in grey.

of structural OH^-, and substantial substitution of PO_4^{3-} by CO_3^{2-} in the apatite lattice. However, a comparison with the synthetic hydroxyapatatie demonstrates that they are within the limits of moderately recrystallized bioapatite. These changes can be related to a prolonged period of diagenetic alteration of the PChMts bones in an aqueous (marine) environment.

Evolution and palaeobiogeography

Penguins have inhabited the Antarctic continent since the Paleocene (Jadwiszczak 2009) and it has been obvious that a 35-million-year gap in their fossil record (Oligocene–Pleistocene) would be sooner or later shrunk. The first record of a fossil bird from East Antarctica, a pseudodontorn (Pelecaniformes, Pelagornithidae) from the Mount Discovery area of McMurdo Sound, was reported by Jones (2000). The bones presented here are the first findings attributable to Sphenisciformes collected within East Antarctica (and also south of the Antarctic Circle). Moreover, they are among the oldest fossils assignable to the extant genus *Spheniscus* (Fig. 7; Göhlich 2007, Stucchi 2007, Ksepka & Thomas 2012), a taxon with its fossil record so far known solely from South America (Jadwiszczak 2009, Ksepka & Thomas 2012).

Based on optimization of breeding ranges from the results of combined analysis of morphology and mitochondrial sequences, Bertelli & Giannini (2005) proposed that the Australian (Austro-New Zealand) ancestor of *Spheniscus* + *Eudyptula* clade (only modern taxa were considered) dispersed to South America via the trans-Pacific route. This finding was recently supported by parsimony ancestral area reconstructions using the strict consensus tree (extant and fossil taxa analysed) but not by those obtained from the Bayesian method (Ksepka & Thomas 2012). In any case, both teams agree that the ancestor of the genus *Spheniscus* most probably lived in South America (Bertelli & Giannini 2005, Ksepka & Thomas 2012). Breeding ranges of all but one recent representative of this taxon are still restricted to that continent (e.g. Göhlich 2007). The only penguin currently breeding in Africa, *Spheniscus demersus* (L., 1758), arrived there sometime in the interval between the Early Pliocene and Middle Pleistocene (Ksepka & Thomas 2012). Thus, according to the current state of knowledge, the Prince Charles Mountains penguin represents an earlier (most probably eastward) dispersal from South America, which strongly suggests that East Antarctica may have played an important role in the evolution of penguins during the Neogene. It may have been an intermediate stop for some lineages (see Ksepka & Thomas 2012, fig. 2) before reaching southern Africa.

Bone morphology suggests that the Fisher Massif penguin most probably was an adult bird, however, whether it was vagrant to the Lambert embayment (possibly in search for food) or returning to breeding grounds, remains unclear. Certainly, the ice retreat may have influenced both vital-for-sphenisciforms environments (i.e. land and sea) resulting in a better access to the potential breeding places and food. The Prydz Bay area is heavily occupied by birds at present. Nine resident and 15 non-resident species have been recognized there, and their populations amount to more than four and two million individuals during breeding season, respectively (Woehler 1997). There is no reason to assume that, at least periodically, the situation was different in the Miocene.

Conclusions

Fossil penguin bones collected from the Fisher Bench Formation (Prince Charles Mountains) belonged to an adult bird from an extinct species of the genus *Spheniscus*. In our estimation, they represent an undescribed taxon, however, the scarcity of the material (solely humerus and radius available) does not make it possible to erect a new species. Both the diatom biostratigraphy and Strontium Isotope Stratigraphy indicate a Late Miocene age for the bones. The co-occurrence of penguin remains and pectenoid bivalves in a marine bank deposit as well as the presence of the shallow-water diatoms nearby (within the same horizon) suggests a deep retreat of the ice sheet in the Lambert embayment associated with a marine incursion.

The bones from the Fisher Bench Formation show diagenetic recrystallization and neoformation, although within the limits of moderately altered bioapatite. These changes reflect diagenetic alteration of the bones in a marine environment. They suggest that the bones experienced prolonged exposition at sea bottom before the final burial in sediment.

The studied penguin inhabited East Antarctica after the MMCT (pronounced cooling) that certainly post-dated the onset of the Antarctic Circumpolar Current. Hence, it had to cope with environmental conditions comparable to those constraining modern Antarctic sphenisciforms. Since the Prince Charles Mountains penguin is geologically older

https://doi.org/10.1017/S0954102012000909 Published online by Cambridge University Press

than the earliest remains attributable to a sole extant representative of African Sphenisciformes (representing the same, i.e. *Spheniscus*, lineage), it seems highly probable that East Antarctica played an important role in the evolution of these birds during the Neogene. More fossils are needed to refine current understanding of the early evolution of extant penguin genera and its relationships to changing climate.

Acknowledgements

The authors are grateful to Valery Lukin, Leader of the Russian Antarctic Expedition (RAE), for inviting Polish geoscientists to participate in the 53rd RAE to East Antarctica in 2008. Field companionship of all members of the geology team led by Dmitry Bolshiyanov in the Prince Charles Mountains is greatly appreciated. Bożena Łącka and Michał Kuźniarski at the Institute of Geological Sciences, Polish Academy of Sciences are thanked for processing the XRD and FTIR data. A photograph of the pectenoid shell was kindly provided by Andrzej Gaździcki (Institute of Paleobiology, Polish Academy of Sciences). The authors greatly appreciate helpful reviews by Steven Emslie and Marcelo Reguero. The study was supported by a research grant of the Polish Ministry of Science and Higher Education no. MNiSW 743/N-Rosja/2010/0, aimed towards scientific collaboration between Poland and Russia in the fields of Antarctic research.

References

Acosta Hospitaleche, C. & Reguero, M. 2010. First articulated skeleton of *Palaeeudyptes gunnari* from the late Eocene of Isla Marambio (Seymour Island), Antarctica. *Antarctic Science*, **22**, 289–298.

Bertelli, S. & Giannini, N.P. 2005. A phylogeny of extant penguins (Aves: Sphenisciformes) combining morphology and mitochondrial sequences. *Cladistics*, **21**, 209–239.

Billups, K. & Schrag, B.P. 2002. Paleotemperatures and ice volume of the past 27 myr revised with paired Mg/Ca and $^{18}O/^{16}O$measurements on bentic foraminifera. *Paleoceanography*, 1029-2000PA000567.

Clarke, J.A., Olivero, E.B. & Puerta, P. 2003. Description of the earliest fossil penguin from South America and first Paleogene vertebrate locality of Tierra del Fuego, Argentina. *American Museum Novitates*, **423**, 1–18.

Clarke, J.A., Ksepka, D.T., Salas-Gismondi, R., Altamirano, A.J., Shawkey, M.D., D'alba, L., Vinther, J., Devries, T.J. & Baby, P. 2010. Fossil evidence for evolution of the shape and color of penguin feathers. *Science*, **330**, 954–957.

Emslie, S.D. & Correa, C.G. 2003. A new species of penguin (Spheniscidae: *Spheniscus*) and other birds from the late Pliocene of Chile. *Proceedings of the Biological Society of Washington*, **116**, 308–316.

Frakes, L.A., Francis, J.E. & Syktus, J.I. 1992. *Climate modes of the Phanerozoic*. Cambridge: Cambridge University Press, 288 pp.

Göhlich, U.B. 2007. The oldest fossil record of the extant penguin genus *Spheniscus* - a new species from the Miocene of Peru. *Acta Palaeontologica Polonica*, **52**, 285–298.

Hambrey, M.J. & McKelvey, B.C. 1991. Neogene fjordal sedimentation on the western margin of the Lambert Graben, East Antarctica. *Sedimentology*, **47**, 577–607.

Howarth, R.J. & McArthur, J.M. 1997. Statistics for strontium isotope stratigraphy: a robust LOWESS fit to the marine Sr-isotope curve for 0 to 206 Ma, with look-up table for derivation of numeric age. *Journal of Geology*, **105**, 441–456.

Huertas, A.D., Iacumin, P. & Longinelli, A. 1997. A stable isotope study of fossil mammal remains from Paglicci Cave, southern Italy, 13 to 33 ka BP: palaeoclimatological considerations. *Chemical Geology*, **141**, 211–223.

Jadwiszczak, P. 2006. Eocene penguins of Seymour Island, Antarctica: taxonomy. *Polish Polar Research*, **27**, 3–62.

Jadwiszczak, P. 2009. Penguin past: the current state of knowledge. *Polish Polar Research*, **30**, 3–28.

Jones, C.M. 2000. The first record of a fossil bird from East Antarctica. *Antarctic Research Series*, **76**, 359–364.

Ksepka, D.T. & Thomas, D.B. 2012. Multiple Cenozoic invasions of Africa by penguins (Aves, Sphenisciformes). *Proceedings of the Royal Society*, **B279**, 1027–1032.

Ksepka, D.T., Bertelli, S. & Giannini, N.P. 2006. The phylogeny of the living and fossil Sphenisciformes (penguins). *Cladistics*, **22**, 412–441.

Layba, A.A. & Pushina, Z.V. 1997. Cenozoic glacial-marine sediments from the Fisher Massif (Prince Charles Mountains). *In* Ricci, C.A., *ed*. *The Antarctic region: geological evolution and processes*. Siena: Terra Antarctica, 977–984.

Lewis, A.R., Marchant, D.R., Ashworth, A.C., Hedenäse, L., Hemming, S.R., Johnson, J.V., Leng, M.J., Machlusf, M.L., Newtoni, A.E., Lan Raine, J., Willenbring, J.K., Williams, M. & Wolfe, A.P. 2008. Mid-Miocene cooling and the extinction of tundra in continental Antarctica. *Proceedings of the National Academy of Sciences of the United States of America*, **105**, 10 676–10 680.

McArthur, J.M., Howarth, R.J. & Bailey, T.R. 2001. Strontium isotope stratigraphy: LOWESS version 3: best fit to the marine Sr-isotope curve for 0–509 Ma and accompanying look-up table for deriving numerical age. *Journal of Geology*, **109**, 155–170.

McKelvey, B.C., Hambrey, M.J., Harwood, D.M., Mabin, M.C.G., Webb, P.-N. & Whitehead, J.M. 2001. The Pagodroma Group - a Cenozoic record of the East Antarctic ice sheet in the northern Prince Charles Mountains. *Antarctic Science*, **13**, 455–468.

Munro, L.E., Longstaffe, F.J. & White, C.D. 2007. Burning and boiling of modern deer bone: effects on crystallinity and oxygen isotope composition of biogenic phosphate. *Palaeogeography, Palaeoecology, Palaeoclimatology*, **249**, 90–102.

Myrcha, A., Jadwiszczak, P., Tambussi, C.P., Noriega, J.I., Gaździcki, A., Tatur, A. & Del Valle, R.A. 2002. Taxonomic revision of Eocene Antarctic penguins based on tarsometatarsal morphology. *Polish Polar Research*, **23**, 5–46.

O'Brien, P.E., Cooper, A.K. & Richter, C. *et al*. 2001. *Proceedings of the Ocean Drilling Program. Initial Reports*, **188**. College Station, TX: Ocean Drilling Program, 10.2973/odp.proc.ir.188.2001.

Panda, R.N., Hsieh, M.F., Chung, R.J. & Chin, T.S. 2003. FTIR, XRD and solid state NMR investigation of carbonate containing hydroxyapatite nano-particles synthesized by hydroxide-gel technique. *Journal of Physics and Chemistry of Solids*, **64**, 193–199.

Person, A., Bocherens, H., Mariotti, A. & Renard, M. 1996. Diagenetic evolution and experimental heating of bone phosphate. *Palaeogeography, Palaeoclimatology, Palaeoecology*, **126**, 135–149.

Person, A., Bocherens, H., Saliège, J-F., Paris, F., Zeitoun, V. & Gérard, M. 1995. Early diagenetic evolution of bone phosphate: an X-ray diffractometry analysis. *Journal of Archaeological Science*, **22**, 211–221.

Pushina, Z.V., Gogorev, R.M., Birjukov, A.S., Egorov, M.S. & Gola, M. 2011. Biostratigraphy of Neogene sediments from the Fisher Massif (Prince Charles Mountains) based on diatom data. *Russian Earth Science Research in Antarctica, Collection of Papers*, **3**, 76–88.

SHEVENELL, A.E., KENNETT, J.P. & LEA, D.W. 2004. Middle Miocene Southern Ocean cooling and Antarctic cryosphere expansion. *Science*, **305**, 1766–1770.

SLACK, K.E., JONES, C.M., ANDO, T., HARRISON, G.L., FORDYCE, R.E., ARNASON, U. & PENNY, D. 2006. Early penguin fossils, plus mitochondrial genomes, calibrate avian evolution. *Molecular Biology and Evolution*, **23**, 1144–1155.

SNEDDEN, J.W. & LIU, C. 2010. A compilation of Phanerozoic sea level change, coastal onlaps and recommended sequence designations. *American Association of Petroleum Geologists. Search and Discovery*, *article no.* 40594. (http://www.searchanddiscovery.com).

STEPHAN, B. 1979. Vergleichende Osteologie der Pinguine. *Mitteilungen aus dem Zoologischen Museum Berlin*, **55** (Supplement Annalen für Ornithologie 3), 3–98.

STUCCHI, M. 2007. Los pingüinos de la formación Pisco (Neógeno), Perú. *Cuadernos del Museo Geominero*, **8**, 367–373.

SUROVELL, T.A. & STINER, M.C. 2001. Standardizing infrared measures of bone mineral crystallinity: an experimental approach. *Journal of Archaeological Science*, **28**, 633–642.

THOMAS, D.B., KSEPKA, D.T. & FORDYCE, R.E. 2010. Penguin heat-retention structures evolved in a greenhouse Earth. *Biology Letters*, **7**, 461–464.

WHITEHEAD, J.M., HARWOOD, D.M. & MCMINN, A. 2003. Ice-distal Upper Miocene marine strata from inland Antarctica. *Sedimentology*, **50**, 531–552.

WHITEHEAD, J.M., QUILTY, P.G., MCKELVEY, B.C. & O'BRIEN, P.E. 2006b. A review of the Cenozoic stratigraphy and glacial history of the Lambert Graben-Prydz Bay region, East Antarctica. *Antarctic Science*, **16**, 83–99.

WHITEHEAD, J.M., HARWOOD, D.M., MCKELVEY, B.C., HAMBREY, M.J. & MCMINN, A. 2004. Diatom biostratigraphy of the Cenozoic fjordal Pagodroma Group, northern Prince Charles Mountains, East Antarctica. *Australian Journal of Earth Sciences*, **51**, 521–547.

WHITEHEAD, J.M., EHRMANN, W., HARWOOD, D.M., HILLEBRAND, C.D., QUILTY, P.G., HART, C., TAVIANI, M., THORN, V. & MCMINN, A. 2006a. Late Miocene paleoenvironment of the Lambert Graben embayment, East Antarctica, evident from: mollusc paleontology, sedimentology and geochemistry. *Global and Planetary Change*, **50**, 127–147.

WOEHLER, E.J. 1997. Seabird abundance, biomass and prey consumption within Prydz Bay, Antarctica, 1980/1981–1992/1993. *Polar Biology*, **17**, 371–383.

ZACHOS, J., PAGANI, M., SLOAN, L., THOMAS, E. & BILLUPS, K. 2001. Trends, rhythms, and aberrations in global climate 65 Ma to present. *Science*, **292**, 686–693.